# Intrinsic edge-localized mode mitigation via Alfvénic turbulence-driven zonal flows in tokamak plasmas

G.Q. Xue[1,2], X.L. Zou[3], W.L. Zhong[1*], Z.X. Wang[2*], R. Ke[1], A.S. Liang[1], G.L. Xiao[1], Y.R. Zhu[1], S.Q. Wang[1], X.L. Zhu[1], Z.C. Yang[1], Y.Q. Shen[1], C.Y. Wang[1], T.F. Sun[1], H.L. Wei[1], M. Jiang[1]

[1] *Southwestern Institute of Physics, Chengdu, China*

[2] *Dalian University of Technology, Dalian, China*

[3] *CEA, IRFM, Saint-Paul-Lez-Durance, France*



The high-confinement mode (H-mode), first discovered in ASDEX in 1982 [1], has become the optimized operating regime for ITER and future fusion reactors due to its ability to sustain steep edge pressure gradients and reduce turbulent transport through the formation of an edge transport barrier (ETB). However, H mode is typically accompanied by edge-localized modes (ELMs) [2], transient instabilities that periodically eject energy and particles toward the plasma-facing components (PFCs) [3]. Developing robust ELM control strategies is critical for advancing magnetic confinement fusion devices. On the one hand, small-ELM or ELM-free regimes—such as quiescent H-mode [4], EDA H-mode [5], QCE H-mode [6] and I-mode [7]—have been explored in various tokamaks experiments. On the other hand, external actuators have been employed to control ELM frequency and mitigate energy loss, including resonance magnetic perturbations (RMP) [8], pellet pacing [9], low Z impurity injection [10], supersonic molecular beam injection (SMBI) [11]and RF heating [12]. These efforts have achieved partial success in suppressing or mitigating ELMs, but often at the cost of added complexity or confinement degradation.

In this paper, we report the observation of high-frequency turbulence during ELM events in the HL-2A tokamak and identify its role in ELM mitigation process. The turbulence exhibits temporal evolution and correlation properties consistent with Alfvénic turbulence and is closely linked to ELM-induced fast-ion redistribution. Our results suggest that this

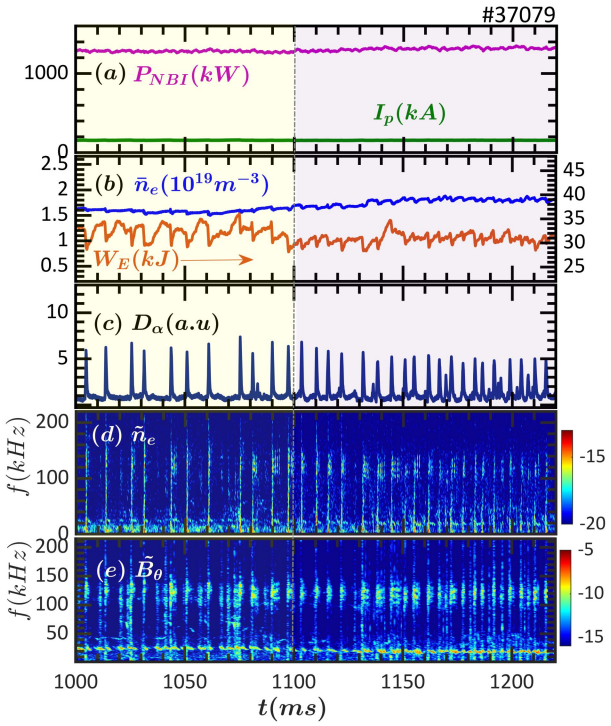


Figure 1. Time evolutions of key plasma parameters for typical H mode plasma. (a) line-averaged electron density, (b) plasma stored energy, (c) $D_\alpha$ intensity, (d) spectrogram of density fluctuation measured by BES at the pedestal region, (e) spectrogram of magnetic perturbation measured by Mirnov probes at the mid-plane.

Alfvénic turbulence drives low-frequency zonal flows, thereby enhancing pedestal transport and reducing ELM energy losses. This self-regulating process operates without any external actuator, revealing a new pathway for ELM control.

Figure 1 presents a discharge exhibiting different ELM behaviours in HL-2A tokamak, which are separated by the vertical dashed line. The left and right shaded regions correspond to different ELM regimes. In this discharge, the sole source of auxiliary heating is NBI, delivering a total heating power of 1.1 MW (figure 1(a)). As shown in the $D_\alpha$ intensity signal in Figure 1(c), the ELMs occurring in the left region exhibit slightly higher amplitudes compared to those in the right region. ELM frequency increases by 2-3 times after 1100ms. Additionally, the associated variations in plasma stored energy (figure 1(b)) are more pronounced in the left region, indicating stronger perturbations during these ELM events. The plasma stored energy loss ( $\Delta W/W$ ) associated with each ELM decreases with the ELM frequency increases, consistent with the empirical trend observed on JET, where ELM energy loss is inversely proportional to ELM frequency. For clarity and consistency in the subsequent analysis, the ELMs in the left region are defined as large ELMs, and those in the right region as small ELMs, unless otherwise specified. Figure 1(d) presents the spectrogram of density fluctuations measured by the BES system and Figure 1(e) shows the spectrogram of magnetic fluctuations measured by magnetic pickup coils located at the outer mid-plane.

Figures 2 (a1–d1) and 2 (a2–d2) provide a comparative visualization of turbulence behavior during two distinct time periods characterized by large and small ELM activity, respectively. Figure 2(c1) shows the integral turbulence intensity across different frequency bands during the large ELM burst, where both a low-frequency turbulence (LFT, 20~60 kHz) and a high-frequency turbulence (HFT,100~150 kHz) occur nearly simultaneously. In contrast, during the small ELM phase, a noticeable time delay is observed between the onset of LFT and HFT, with the latter lagging behind, as shown in Figure 2(c2). Figures 2(d1) and 2(d2) illustrate the temporal evolution of the pedestal electron density gradient in response to the ELM crash and subsequent

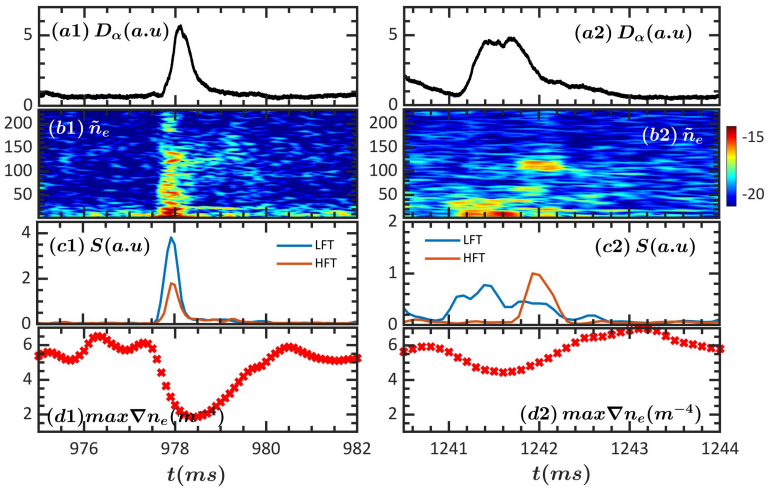


Figure 2. Comparison of plasma edge dynamics during a large ELM (left, a1–d1) and a small ELM (right, a2–d2). (a1, a2) Dα signals, (b1, b2) spectrogram of density fluctuation, (c1, c2) integrated turbulence intensity in 20–60 kHz (blue) and 100–150 kHz (orange) bands; (d1, d2) maximum electron density gradient at pedestal region.

recovery. Figure 2(d2) demonstrates that the maximum density gradient recovers more rapidly when a longer delay is observed in the onset of HFT. These observations suggest that high-frequency turbulence, potentially modulated by the delay time relative to LFT onset, plays a role in regulating particle transport in the pedestal region.

Figure 3 presents the the correlation between the time delay ($\Delta\tau$) of LFT and HFT, and the normalized stored energy loss ($\Delta W/W$ during ELM events. Here, $\Delta W/W$ is used as a quantitative proxy for the ELM size. The data points were obtained from multiple ELMy H-mode discharges. It has been shown that greater $\Delta W/W$ , that is, larger ELMs, are associated with shorter $\Delta\tau$. This suggests that longer delay times may contribute to a mitigation of ELM-induced energy losses. It can be considered that the recovery time of the plasma pedestal following an ELM crash is found to be shorter for smaller ELMs, implying that a longer delay is correlated with faster particle transport. These results suggest a possible interplay between turbulence dynamics and ELM crash behavior. In particular, the HFT appears to regulate the rate of pedestal recovery following ELM crashes via turbulent transport mechanisms. Overall, the observed inverse relationship between delay time and ELM energy loss demonstrates the potential of exploiting turbulence dynamics for reduced ELM energy losses and pedestal performance optimization.

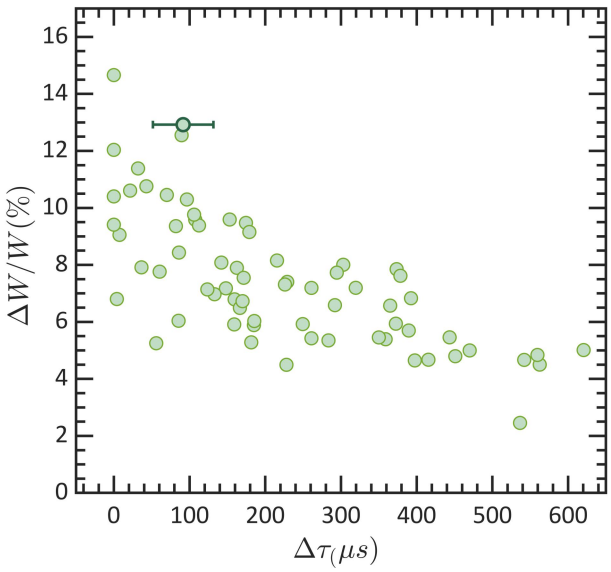

Figure 3. Energy loss caused by ELM against the time delay of the HFT and LFT.

The characteristics of the HF mode during ELMs are analysed using the BES system. The mode is found to propagate in the ion diamagnetic drift direction, with a poloidal wavenumber of $k_\theta$~0.4 $cm^{-1}$. We propose that the high-frequency turbulence, observed with a time delay during ELM bursts, could be Alfvénic turbulence driven by the redistribution and acceleration of fast ions induced by the ELM crash. This hypothesis is inferred from theoretical considerations and supported by the turbulence's frequency alignment with the toroidal Alfvén eigenmode (TAE) gap.

To investigate the interplay between the alfvenic turbulence and background turbulence, bi-spectrum analysis is employed. The figure 4 (a) displays the auto-bispectrum of the density fluctuations at the pedestal region measured by BES. The spectrum is evaluated over the time window of 1250 – 1300ms, corresponding to concatenated ELM bursts, during which a pronounced delay is observed between the HFT and the LFT. The color scale in figure 4(a) represents the magnitude of bispectrum, indicating the strength of nonlinear phase coupling

among frequency triplets satisfying $f_3 = f_1 \pm f_2$ . The bispectrum distinctly reveals pronounced broadband peaks at $(f_1, f_2) = (f_{AT}, 0)$ and $(f_{AT}, -f_{AT})$, indicating a phase-matched nonlinear coupling between Alfvénic turbulence and near-zero-frequency zonal flow (LFZF). Figure 4(b) displays a one-dimensional slice of the bispectrum at $f_2 = 0kHz$, providing a qualitative characterization of the three-wave coupling amplitude. The peak observed corresponds to the generation of LFZF by fast-ion-driven Alfvénic turbulence, following the three-wave coupling condition $f_{AT} - f_{AT} = f_{LFZF}$ . Such LFZF – turbulence coupling plays a key role in regulating turbulent transport in magnetic plasmas. The zonal flow effectively reduces the radial correlation length of Alfvénic turbulence, thereby significantly suppressing turbulent transport and the associated energy losses at the plasma edge. Consequently, this turbulence suppression mechanism directly facilitates the formation of smaller, less energy loss ELMs.

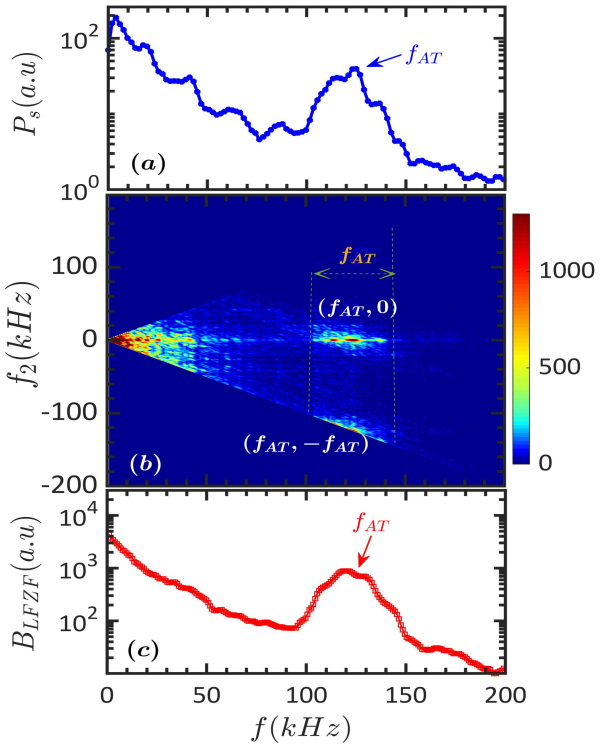


Figure 4. Auto-power spectrum (a), auto bi-spectrum (b) and the slice (c) of the density fluctuation at the pedestal region measured by BES.

Our findings not only provides deeper insights into ELM mitigation but also opens pathways for targeted manipulation of fast-ion populations and turbulence dynamics in future fusion reactor scenarios.



## References


[1] F. Wagner et al., Phys. Rev. Lett. 49, 1408 (1982).

[2] H. Zohm, Plasma Phys. Control. Fusion 38, 105 (1996).

[3] G. Federici et al., Nucl. Fusion 41, 1967 (2001)

[4] K. H. Burrell et al., Phys. Plasmas 8, 2153 (2001).

[5] M. Greenwald et al., Phys. Plasmas 6, 1943 (1999).

[6] M. Faitsch et al., Nucl. Mater. Energy 26, 100890 (2021).

[7] D.G. Whyte et al., Nucl. Fusion 50, 105005 (2010).

[8] T. E. Evans et al., Nucl. Fusion 48, 024002 (2008).

[9] P. T. Lang et al., Phys. Rev. Lett. 79, 1487 (1997).

[10] W. L. Zhong et al., Rev. Sci. Instrum. 85, 013507 (2014).

[11] W. W. Xiao et al., Nucl. Fusion 54, 023003 (2014).

[12] G. L. Xiao et al., Nucl. Fusion 59, 126033 (2019).